Numerical Magneto Hydro Dynamic Flow Simulation of Velocity and Pressure for Electrically Conducting, Incompressible Fluids

Raoudha Chaabane
Raoudha.Chaabane@issatgb.rnu.tn
Raoudhach@yahoo.fr
Laboratoire d'Etudes des Systèmes Thermiques et Energétiques
Ecole Nationale des Ingénieurs de Monastir
Av. Ibn ElJazzar 5019 Monastir, Tunisia

Adam Bouras

Sassi Ben Nasrallah

In this paper, we report on numerical simulations of incompressible MagnetoHydroDdynamic flows by a two dimensional finite difference scheme associated to an appropriate projection method performed to characterize velocity-pressure formulations along the specified MHD duct by solving the set of differential equations of magnetohydrodynamics. In the present calculation, a working electrolytic solution is considered in order to bring up the application of the magnetohydrodynamic micropump. Numerical results show the characteristics of flow velocity, pressure distribution and their convergence tests. The computations aim to optimize the flow rate of a given MHD micropump regarding to its geometrical dimensions and the external electromagnetic excitation.
***Keywords**: magneto-hydrodynamics equations, Lorentz force, finite difference scheme, projection method, velocity-pressure formulation.*

Introduction

The determination of velocity and pressure fields in fluids is an important problem in a number of technological applications based on flows of conducting fluids through channels of various cross-sections. In practice, there is a great need to understand the effect of an external body force, on the conducting fluid in two dimensional, time dependant situations. Here, a finite difference scheme will be described which is suitable for use on a microcomputer and which can solve a range of magnetohydrodynamic flows where magnetic field is independent of the flow as enumerated by Cramer (1973) in the analogy applied between the magnetic field equation and the vorticity equation. So the governing equations of the MHD micropump will be derived under a negligible magnetic Reynolds number.

Along the specified duct, we consider for the time being, a single-phase fluid homogeneous incompressible MHD equation in a two-dimensional bounded domain. This paper outlines the investigation of the fundamental performance of a linear Faraday type MHD micropump using an electrolytic working solution where its performance is characterized using two-dimensional finite numerical simulation with an appropriate projection method. The numerical simulation is carried out on the basis of the MHD equations, (mass and momentum equations including MHD effects) and the set of Maxwell equations developed by Kadid, (2004). And, in order to solve this set of equations, the Taylor expansion is used, which is one of the finite difference methods using an artificial viscosity under initial conditions of isentropic flow.

Magnetohydrodynamics involves then a combination of both electrical and magnetic fields in order to induce mechanical flow in a fluid that is made conductive by dissolving an electrolyte in it. Since the ionic flow in the magnetic field is the cause of the movement of the conductive fluid, then it is necessary to understand the properties of the electromagnetic forces at work. So, over the last decade, considerable efforts have been directed to the possibility of using MHD technology for pumping system, where electrical energy is converted directly into force on the working solution. In recent works of Harada et all (2002) and Anwari (2005), the basic characteristics of a linear Faraday type MHD accelerator were studied, both theoretically and numerically, for various loading configurations.

In the case of electrolytic solutions, the moving ions drag fluid molecules with them. These new possibilities of carrying out the fluid particles are presented in Kim et all (1997), Ben Salah (1999) and Jang et all (2000) works where they try to conceive a magnetohydrodynamic system aiming to induce continuous pumping of a conductive fluid without the presence of any moving parts, advantages enumerated by Lemoff et all in (2000) and later by Homsy et all (2005). These last fields of research define the Magneto-Hydro-Dynamic acceleration concept where the mechanical force of flow is induced on a conductive fluid when it is excited by an electromagnetic field, Jang et all (2000).

This document is organized in five sections. The first section is devoted to the magnetohydrodynamic pumping theory. In the second section, the magneto hydrodynamic modeling is highlighted. Section three is concerned with the mathematical model to solve the classical configuration problem based on the magnetohydrodynamic governing equations. Discrete equations are introduced in the section four. The projection method and the numerical procedure are the subject of ongoing work. Finally, numerical results discussion is presented.

Paper accepted October, 2007. Technical Editor: Francisco R. Cunha.

Nomenclature

$\mathbf{B}$ = *magnetic flux density, T*
d = *grid size of cell, m*
$\mathbf{E}$ = *electric field, N/C*
f = *frequency, Hz*
$\mathbf{F}$ = *Lorentz force, N*
F_+ = *Lorentz force carried by positive ions, N*
F_- = *Lorentz force carried by negative ions, N*
h = *height of the electrode, m*
Ha = *Hartmann number, dimensionless*
I = *electric current, A*
J = *electric current density, A/m²*
k = *constant*
ℓ = *distance between electrodes, m*
Le = *total length of the MHD channel, m*
L = *Characteristic length of the fluid flow, m*
n = *normal direction*
N = *interaction parameter dimensionless*

N_α = *number of ions of species* α *in the duct*
p = *pressure, N/m²*
$\bar{p}$ = *average pressure over the width of the outlet duct, N/m²*
q = *unit charge, 1.6 10^{-19} C*
Re = *hydrodynamic Reynolds number, dimensionless*
S =*cross sectional area of channel, m²*
s = *threshold of convergence*
t = *time, s*
Δt =*time step, s*
U = *velocity, m/s*
$\bar{u}$ = *average velocity over the width of the outlet duct, m/s*
u_n = *normal velocity, m/s*
u_t = *tangential velocity, m/s*
u = *component of dimensional velocity in the x-axis direction, m/s*
v = *component of dimensional velocity in the y-axis direction, m/s*
U =*Characteristic velocity of the fluid flow, m/s*
V = *total volume device, m³*
x = *axis in Cartesian coordinates*
y = *axis in Cartesian coordinates*
z = *axis in Cartesian coordinates*
z_α = *valence of ions of species* α *in the duct*

Greek Symbols

ν = kinematic viscosity of the fluid, m²/s
σ =electrical conductivity, 1/(Ω.m)
φ = phase shift, rad
μ_j = electrophoretic mobility, m²/(V s)
μ = fluid dynamic viscosity Kg /(m s)
ρ =flow density, Kg/m³
ϑ =flow velocity, m/s
Φ =electric potential, volt

Superscripts

n relative to variable evaluated at time t
n+1 relative to variable evaluated at time t+ Δt

Subscripts

i relative to direction of the axis in the system of coordinates or component
j relative to direction of the axis in the system of coordinates or component

Abbreviation

MHD relative to MagnetoHydroDynamic
MEMS relative to Micro Electro Mechanical Systems
< > relative to time average

MHD Pumping Theory

Motion of electrically conducting fluids across a magnetic field induces the so-called Lorentz force. Consider a rectangular cross-section duct filled with an electrolyte solution where a homogeneous electrical field E is applied between the sidewalls consisting of an electrically conductive material, as shown in Fig. 1. In order to manage the flow movement, a homogeneous magnetic flux density is applied perpendicular to both the duct length axis and the electrical field.

This force applied on every ion of species α in the electrolyte solution is expressed by Feynman (1964) as

$$F_\alpha = q.z_\alpha.(E + \vartheta_\alpha \wedge B) \tag{1}$$

The applied electrical field yields electrical forces, which act in opposite direction for ions of opposite charge (see Fig.1)

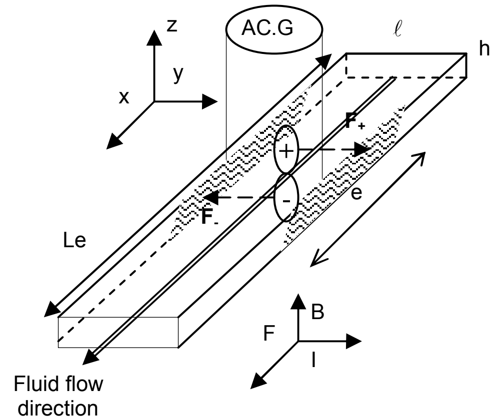

Figure 1. Vector diagram of MHD pump and electrical forces exerted in solution's ions.

Assuming that N_α is the number of ions of species α in the MHD duct and due to the electroneutrality of the bulk solution, there is no net electric force exerted on the solution by the electric field, thus

$$q.E\sum_\alpha z_\alpha.N_\alpha = 0 \tag{2}$$

From equation (1), the total Lorentz force will be defined as

$$q.\sum_\alpha N_\alpha.z_\alpha.\vartheta_\alpha \wedge B \tag{3}$$

So, the Lorentz force is proportional to the velocity of the charge carriers in the plane perpendicular to the magnetic field which can be split into two components

$$\vartheta_\alpha = \vartheta_{\alpha x} + \vartheta_{\alpha y} \tag{4}$$

where $\vartheta_{\alpha x}$ is the velocity parallel to the electric field and $\vartheta_{\alpha y}$ is the velocity parallel to the channel axis. The latter one will induce the Lorentz force which is significant in determining the flow profile based on the dimensionless Hartmann number, given by the ratio of the magnetic body force and the viscous force $Ha = (N.Re)^{1/2}$, where $N = \sigma.L.B^2 / \rho.U$ stands for the non-dimensional interaction parameter and $Re = UL/\nu$ is the non-dimensional hydrodynamic Reynolds number, so the Hartmann number can be rewritten as Ha= $L.B.(\sigma / \mu)^{1/2}$ where the dynamic viscosity μ is expressed as $\rho\nu$.

Table 1. Properties of seawater (20° C, 1 atm); Jang and Lee (2000); Liu et all (2006).

ρ	Density = 1025 Kg/m³
μ	Dynamic viscosity = 1.09 10^{-3} Kg /(m s)
ν	Kinematic viscosity = 1.0634 10^{-6} m² /s
μ_0	Magnetic permeability of the free space = $4\pi.10^{-7} H/m$
σ	Electrical conductivity = 4 $1/(\Omega m)$
η	Diffusivity = 1.98 10^5 $(\Omega.m^2)/H$

Compared to metals or plasma fluids, the medium is characterized by a constant, poor electric conductivity σ ($\Omega^{-1}m^{-1}$) highlighten a low magnetic Reynolds number Re_m, namely

$$Re_m = UL\sigma\mu_0 = UL/\eta \tag{5}$$

where μ_0 stands for the magnetic permeability of fluid medium equal to the permeability of the free space and η is the medium diffusivity.

The chosen electric conductivity yields to a Hartmann number close to zero due to the low value of σ. This result, allow us to neglect the velocity $\vartheta_{\alpha y}$. As consequence, only the ionic velocity parallel to the electric field will be considered, expressed by $\vartheta_{\alpha x}= \mu_\alpha E$ with μ_α is the electrophoretic mobility. Consequently, the net sum of the Lorentz force on all migrating ions is

$$q.\sum_\alpha N_\alpha.z_\alpha.\vartheta_{\alpha x} \wedge B \tag{6}$$

$$q.\sum_\alpha N_\alpha.z_\alpha.(\mu_\alpha E) \wedge B \tag{7}$$

$$q.E \wedge B\sum_\alpha N_\alpha.z_\alpha.\mu_\alpha \tag{8}$$

Given that the term $q.\sum_\alpha N_\alpha.z_\alpha.\mu_\alpha$ represents the conductivity of the fluid medium multiplied by its volume and referring to our geometry, the Lorentz force can be rewritten as

$$F = \sigma.V.(E \wedge B) = V(J \wedge B) = \ell.(I \wedge B) \tag{9}$$

As presented, the Lorentz force presents a crucial step in a magnetohydrodynamic pumping system, handling conductive fluids, as shown in Homsy et all (2000). Besides, with the recent progress in Micro Electro Mechanical Systems (MEMS) technologies, a large research effort has been made in microfluidic area, in order to pump and precisely control small volumes of small samples, where conductive fluids are propelled using Lorenz force. In (2000), Jang and Lee were the first to fabricate a MHD micropump, designed to propel saline solutions induced by a permanent DC magnet. However, electrochemical decomposition and electrodes degradation disrupted the flow. So, aiming a good pumping and a high flow rate, a permanent AC magnet was used by Heng et all (1999). More recently, Lemoff and Lee (2000) studied MHD pumping with combined AC magnetic fields and an AC current at high frequency.

To prevent gas bubble, electrolysis and electrodes degradation, a sinusoidal electric current and a magnetic flux density will be applied at a same frequency (f), with a suitable phase shift φ leading to the following formula expressing the time average Lorenz force:

$$\langle F \rangle = \ell.f.I.B.\int_0^{1/f} cos(2\pi ft).cos(2\pi f + \varphi)dt \tag{10}$$

Evaluating the integral we obtain

$$\langle F \rangle = 1/2(\ell.I.B\cos\varphi) \tag{11}$$

Equation (11) describes the time average of Lorentz force strength as function of distance between electrodes, magnetic flux density and the applied electric current, indicating that the flow rate, proportional to the Lorentz force measured in the duct, is therefore proportional to the applied current density and magnetic flux density, to the cosine of the phase angle between both, as well as to the micropump channel width. The maximum value of this expression is reached for a phase shift of 2π for a well known external electromagnetic excitation and micropump's geometrical dimensions.

MHD Modeling

The MHD flow is governed by classical fluid dynamics and electromagnetics, including a set of coupled partial differential equations that express the conservation of mass continuity and Navier-Stokes equation joined to the Maxwell's, current continuity and constitutive equations. In this paper, electrically conducting fluid flow constrained in a rectangular MHD duct, where a uniform magnetic field is applied perpendicular to the stream-wise direction and to the homogeneous electric field.

The flow is characterized by a negligible magnetic Reynolds number, which is an usual case with micro-duct flow where magnetic field is independent of the flow from vorticity equation $w = \nabla \wedge \vartheta$ and magnetic field equation as presented by works of Cramer (1973).

With these assumptions and adopting a dimensional analysis based on the characteristic current density $\overline{j}$ of σE and the characteristic pressure $\overline{p}$ of $\mu.U/L$, the governing equations are reduced to the following equations

$$\nabla\overline{\vartheta} = 0 \tag{12}$$

$$\overline{j} = \overline{E} + \frac{(\overline{\vartheta} \wedge \overline{B})}{R_E} \tag{13}$$

$$\frac{\partial\overline{\vartheta}}{\partial t} + \overline{\vartheta}.\overline{\nabla\vartheta} + \frac{1}{R_e}\overline{\nabla p} = \frac{1}{R_e}\overline{\nabla}^2\overline{\vartheta} + N(\overline{j} \wedge \overline{B}) \tag{14}$$

where $R_E = E/UB$, E is the electric field density, B is the characteristic magnetic flux density and U is the characteristic velocity. The parameter R_E has large value in the microchannel in which high electric field is applied, indicating that j is little dependant on the velocity ϑ. This guarantees very small fluctuations of the magnetic field due to the fluid motion as compared to the external applied field, therefore the total magnetic field can be considered uniform and time independent.

In general, the induced electrical current j is given by $j = \sigma(-\nabla\Phi + \vartheta \wedge B)$ where Φ is the induced electrical potential, produced by the interactions of the flow vorticity $w = \nabla \wedge \vartheta$ and the applied magnetic field. Besides, the configuration considered here is two dimensional for which, in practice, it is reasonable to assume that the vorticity is negligible. With this assumption, the induced electrical potential can be assumed to be null as cited in Holman (1990), so the Lorentz force defined per unit of volume, takes the form

$$\mathrm{j} \wedge \mathrm{B} = \sigma(\vartheta \wedge \mathrm{B}) \wedge \mathrm{B} = \sigma.E.B \tag{15}$$

As outlined above, the MHD equations for the transient 2-D (x-y) planar flow with the presence of a uniform, time dependant, positive z-direction magnetic field and y-direction electric field are formulated as

$$\frac{\partial u}{\partial x}+\frac{\partial v}{\partial y}=0 \quad (16)$$

$$\rho\frac{Du}{Dt}=-\frac{\partial p}{\partial x}+\mu(\frac{\partial^2 u}{\partial x^2}+\frac{\partial^2 u}{\partial y^2})+F_x \quad (17)$$

$$\rho\frac{Dv}{Dt}=-\frac{\partial p}{\partial y}+\mu(\frac{\partial^2 v}{\partial x^2}+\frac{\partial^2 v}{\partial y^2})+F_y \quad (18)$$

where u denote the velocity component in the streamwise x-direction and v denote the velocity component in the transverse y-direction, D/Dt is the material derivative, μ is the fluid dynamic viscosity and F_x, F_y are the component of the Lorentz force, per unit volume, in x-direction and y-direction, respectively.

Table. 2 Data and parameters for computer experiment

L=900 µm	Distance between micropump's electrodes
I=0.8 A	Applied electric current
B=0.05 T	Applied magnetic field
Δt =0.1	Time discretization

MHD Governing Equations

In this numerical simulation, we consider the widely used set of basic equations with MHD approximations, as given by eq. (9). Since the essential feature of the MHD flow is the existence of a Lorentz force, fluid equations, eqs. (16-17-18), including MHD effects are used.

Aiming a fundamental performance of the magnetohydrodynamic accelerator, the research employed two-dimensional numerical simulation with a mesh of 40 by 40 grid points. Further, for time discretization, and in order to have a consistent scheme, i.e., with a unique and limited solution, the following condition is used $d^2 \geq 2.\nu.\Delta t$, where d is the cell size.

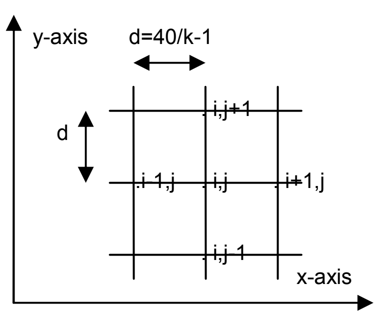

Figure 2. Typical cell for the finite difference scheme

It was assumed that a low viscous, incompressible, conducting fluid is flowing in the x-direction, down z-axis magnetic field and y-axis electric field. In solving the flow field, no slip condition is imposed on the walls of the duct. The velocity boundary condition at the duct walls is the thin conducting wall condition cited in Shercliff (1956), Hunt (1965), Temperley et all (1971) and Tillak et all (1998), where u_n and u_t are the normal and the tangential velocity, respectively.

$$u_n = 0 \quad (19)$$

$$u_t = k.\partial u_t / \partial n \quad (20)$$

The cross-section of the duct having a boundary conditions described for pressure field and satisfying Neumann condition

$$\partial P/\partial n = 0 \quad (21)$$

For the initial condition, the velocity field is considered divergence free and is assumed to satisfy the no-slip boundary condition $u = v = 0$, except in the entrance of the duct. A constant pressure P=0 is defined everywhere in the MHD duct. Figure 3 shows the geometry and boundary conditions, where for the inner MHD duct we adopt a characteristic function equal to the unit and zero elsewhere. However, for the corners the value of the characteristic function is hold at 2 and for the edges it is assumed to be 1 as depicted in figure. 3.

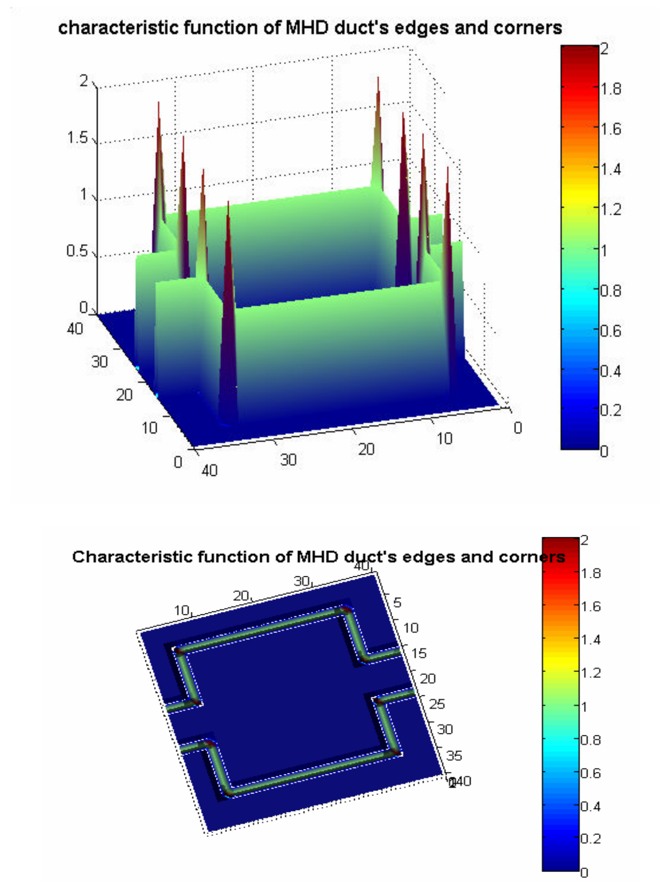

Figure 3. Cavity geometry and characteristic function

For our specific application, it will be supposed that there is a uniform magnetic field imposed in the z-direction and there is a null axial velocity gradient.

Also, an uniform velocity parallel to the duct direction is imposed $U_{(t=0)}$=1. In the outlet duct, we consider a null velocity gradient $\lambda(c_1) = \lambda(c_2)$ where $\lambda = u, v$.

Internal and external corners must satisfy pressure and velocity conditions depicted in figures 4 to 6.

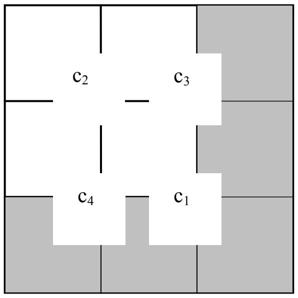

Figure 4. Internal corner $\mathbf{P(c_1) = P(c_2) U(c_1) = 0}$.

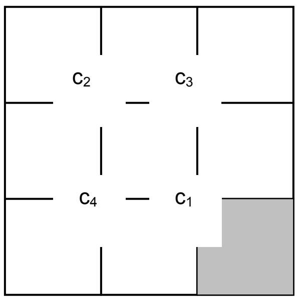

Figure 5. External corner $\mathbf{P(C_1) = 1/2(P(C_3) + P(C_4)) U(C_1) \infty U(C_2)}$.

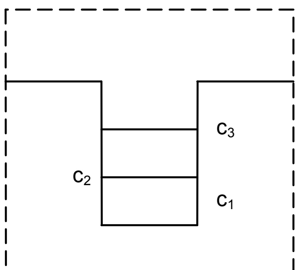

Figure 6. Extrapolation of pressure field $P(c_1) = 2P(c_2) - P(c_3)$.

These conditions are incorporated with the MHD equations governing the magnetohydrodynamic flow.

Discrete Equations

An elementary Taylor expansion for first and second order is used to describe the magnetohydrodynamic equations for

$$\lambda = u, v \quad \frac{\partial \lambda^n}{\partial x_{i,j}} = \frac{\lambda^n_{i+1,j} - \lambda^n_{i-1,j}}{2d} \; ; \frac{\partial \lambda^n}{\partial y_{i,j}} = \frac{\lambda^n_{i,j+1} - \lambda^n_{i,j-1}}{2d} \tag{22}$$

$$\frac{\partial^2 \lambda^n}{\partial {x_{i,j}}^2} = \frac{\lambda^n_{i+1,j} - 2\lambda^n_{i,j} + \lambda^n_{i-1,j}}{d^2} \; ; \frac{\partial^2 \lambda^n}{\partial {y_{i,j}}^2} = \frac{\lambda^n_{i,j+1} - 2\lambda^n_{i,j} + \lambda^n_{i,j-1}}{d^2} \tag{23}$$

$$\frac{\partial p^n}{\partial x_{i,j}} = \frac{p^n_{i+1,j} - p^n_{i-1,j}}{2d} \qquad 24)$$

For time explicit scheme we have

$$\frac{\partial u^n}{\partial t} = \frac{u^{n+1}_{i,j} - u^n_{i,j}}{dt} \tag{25}$$

The discrete equations form shows that the diagonal term coefficient is proportional to viscosity. So, if we work with a low viscous fluid, this term can be neglected and the transport phenomenon will dominate the diffusion one.

In order to equalize the weighted diffusive and convective term, we introduce a numerical viscosity. As result, the convergence criteria aims to minimize the partial derivative of velocity, more precisely $\left|\overline{\lambda}(n) - \overline{\lambda}(n-10)\right| < s$, for n>10 where $s = 10^{-4}$.

Projection Method and Numerical Procedure

Numerical resolution of the momentum equation is incorporated with the continuity equation which must be verified at every time step. Besides, the pressure field deduced from the velocity evolution must satisfy the condition of mass conservation. So, we use a mathematical projection method introduced and developed in the different works of Temam (1977), Chorin (1986), Gerbeau (1997) and Guermond (2003). It consists of two sub-steps per time step where the pressure is treated explicitly in the first sub-step and corrected in the second one by projecting the intermediate velocity onto the space of divergence-free fields.

The time integration of the velocity is rewritten as

$$\frac{\partial \mathrm{U}}{\partial t} = \frac{\mathrm{U}^{n+1} - \mathrm{U}^n}{dt} = \frac{\mathrm{U}^{n+1} - \mathrm{U}^{n+1/2}}{dt} + \frac{\mathrm{U}^{n+1/2} - \mathrm{U}^n}{dt} \tag{26}$$

The prediction step consists of solving the following equation in order to deduce $\mathrm{U}^{n+1/2}$ calculated from U^n

$$\nu.\nabla^2 \mathrm{U} + \frac{F}{\rho} - (\mathrm{U}.\nabla).\mathrm{U} = \frac{\mathrm{U}^{n+1/2} - \mathrm{U}^n}{dt} \tag{27}$$

We consider the pressure field at (t+ Δt), the divergence of the following equation

$$\frac{-\nabla.p}{\rho} = \frac{\mathrm{U}^{n+1} - \mathrm{U}^{n+1/2}}{dt} \tag{28}$$

So, applying divergence to pressure at (t+ Δt) is

$$\nabla.\left(\frac{-\nabla.p^{n+1}}{\rho}\right) = \nabla.\left(\frac{\mathrm{U}^{n+1} - \mathrm{U}^{n+1/2}}{dt}\right) \tag{29}$$

The condition of continuity at (t+ Δt) is written as

$$\nabla.\boldsymbol{U}^{n+1} = 0 \tag{30}$$

The pressure field at (t+ Δt) satisfy Poisson equation model and is rewritten as

$$\frac{\Delta.p}{\rho} = \frac{\nabla.\mathrm{U}^{n+1/2}}{dt} \tag{31}$$

The finite difference scheme for Poisson equation implies

$$\overline{p}^{n+1}(i,j) = \frac{p^{n+1}(i+1,j) + p^{n+1}(i-1,j) + p^{n+1}(i,j+1) + p^{n+1}(i,j-1)}{4} - d^2 \frac{\nabla.\mathrm{U}(i,j)}{4dt} \tag{32}$$

$$\nabla.\mathrm{U}(i,j) = \frac{u^{n+1/2}(i+1,j) - u^{n+1/2}(i-1,j)}{2d} + \frac{v^{n+1/2}(i,j+1) - v^{n+1/2}(i,j-1)}{2d} \tag{33}$$

We complement these equations with a Neumann condition

$$\frac{\partial p}{\partial n} = 0 \tag{34}$$

Having the pressure field, we deduce the velocity evolution satisfying the momentum equation and the continuity one.

$$\mathrm{U}^{n+1} = \mathrm{U}^{n+1/2} - \frac{\nabla . p}{\rho} . dt \tag{35}$$

$$u^{n+1}(i,j) = u^{n+1/2}(i,j) - dt \frac{p^{n+1}(i+1,j) - p^{n+1}(i-1,j)}{2\rho d} \tag{36}$$

$$v^{n+1}(i,j) = v^{n+1/2}(i,j) - dt \frac{p^{n+1}(i,j+1) - p^{n+1}(i,j-1)}{2\rho d} \tag{37}$$

Numerical Results And Discussions

We will now present and analyse the numerical results for the electrolytic solution inside the MHD micropump where we present plots of flow velocity, pressure distribution and convergence tests for both pressure and velocity. The ongoing computation aims to show the characteristic of the MHD flow in a 40*40 mesh. All simulations are realised for the following parameters, a current density of I=0.8A, a magnetic field of B=0.05T and a micropump with a width of ℓ =900 μm . 580 iterations were employed for both pressure and velocity.

The analysis of the obtained results for velocity profile inside the magnetohydrodynamic micropump depicted in figures 7 to 9 shows that velocity in x-axis direction have a constant value along the duct and decrease slightly in the extreme outlet of the channel exit. While velocity in y-axis direction depicted in Fig. 8 present some fluctuations in the entrance of the duct.

Regarding symmetrically to the flow direction, velocity profile presents a minimum followed by a maximum in the right sight of the duct. However, close to the outlet of the magnetohydrodynamic duct the inverse situation is depicted with a more noticeable elevation.

As result, the norm velocity distribution inside the duct, defined as $\sqrt{u^2 + v^2}$, is depicted in fig. 9 indicating a noticeable elevation in the middle of the micropump's channel. So, the velocity study confirms that the working fluid was successfully accelerated by the Lorentz force due to the externally applied current and the magnetic flux density related to the chosen geometry.

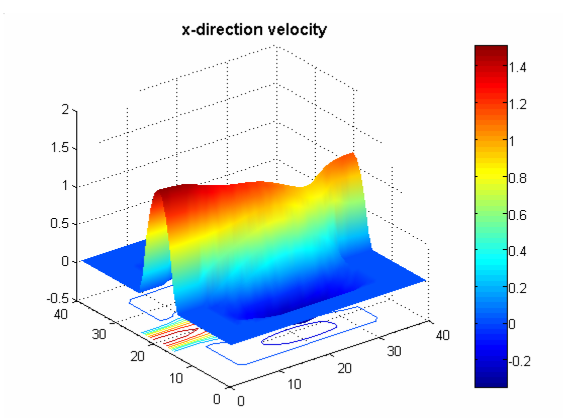

Figure 7. Velocity variation in x-direction

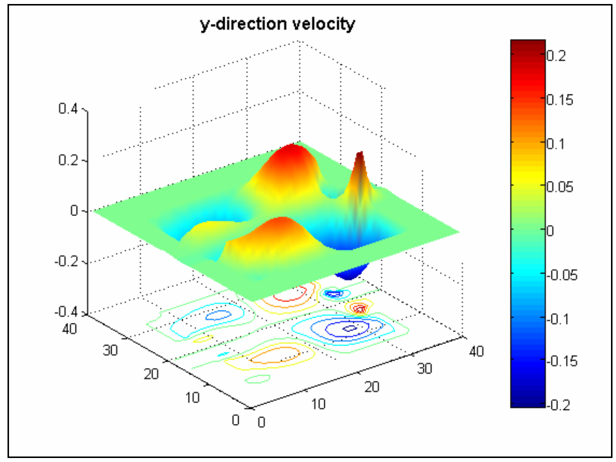

Figure 8. Velocity variation in y-direction

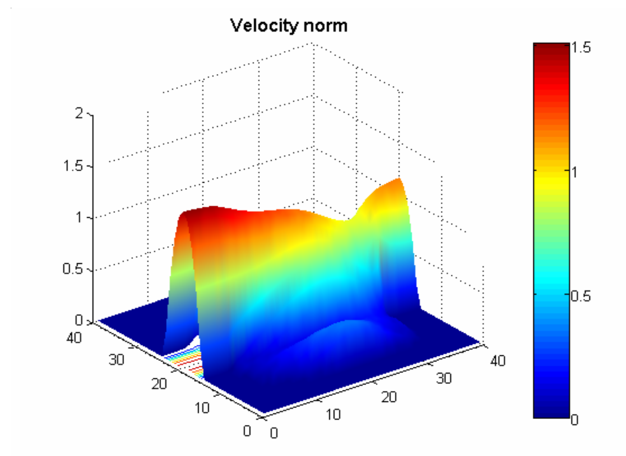

Figure 9. Velocity norm

Focused on the pressure behavior in fig.10, we can notice a noticeable elevation of the pressure in of the inlet of the magnetohydrodynamic duct, followed by a two symmetric diminution equidistant from the x-axis. In the outlet of the duct, the pressure presents a symmetric increase regarding the x-direction. From Figure.10, we can deduce that the imposed inlet and outlet geometry is the essential parameter of the pressure elevation. However, in the middle of the duct, the flow shows a symmetric depression. In order to understand the coupling between the velocity and the pressure, in fig.11, both quantities are presented, i.e., the velocity vector field and isolines of pressure.

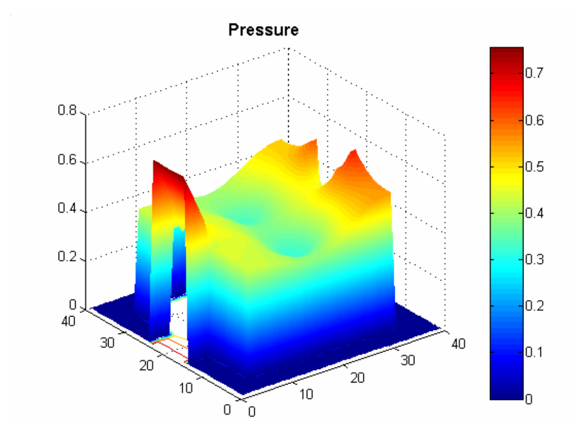

Figure 10. Pressure distribution

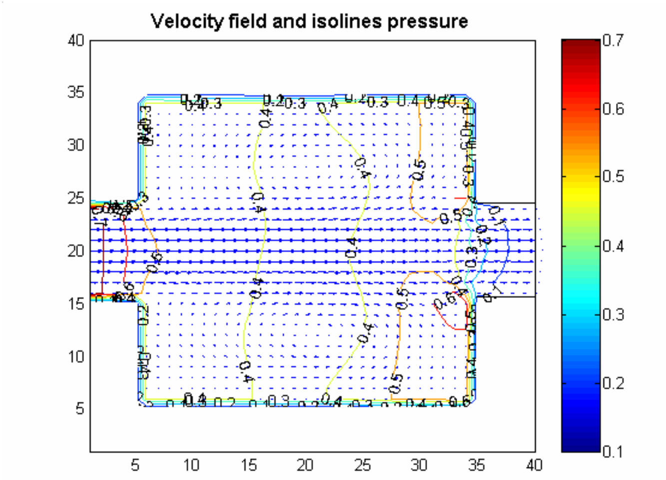

Figure11. Velocity field and isobar plots

At each time step, the pressure and the velocity fields are solved alternatively and iteratively until convergence is reached. The process is repeated until satisfying convergence criteria. Convergence behavior of pressure distribution and field velocity can be depicted in fig. 12 and 13. Such convergence plots prove the efficiency of the numerical approach adopted in this paper.

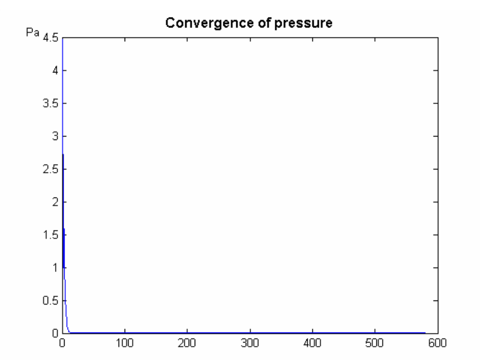

Figure 12. Convergence of pressure distribution

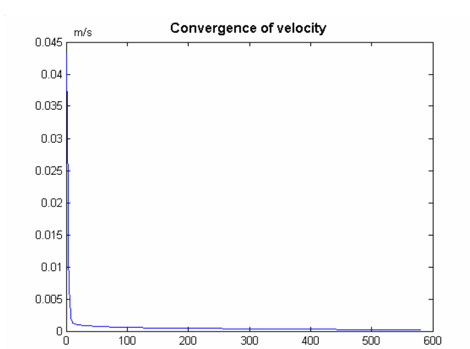

Figure 13. Convergence of velocity field

To summarize, inspection of the flow velocity characteristics shows that the Lorentz force effect has successfully accelerated the electrolytic solution inside the MHD micropump. These results are high lighten in fig.14 by the computation of the flow lines for I=800 mA, B=0.05 T with a chosen distance between electrodes of 9.10^{-4}m.

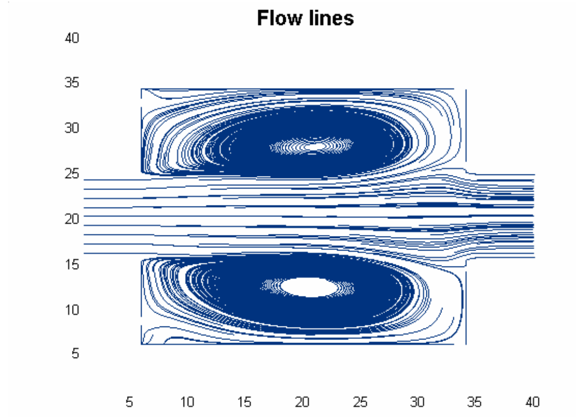

Figure 14. Flow lines for I=0.8A, B=0.05T and e=9.10^{-4}m 580 iterations for velocity and pressure (ip_{max}= iu_{max}=580)

Conclusion

This paper has presented a numerical method based on the performance of a MHD micropump with Faraday electrode configuration evaluated by a two dimensional finite difference scheme. From our results, we concluded that the cited method achieves good convergence for pressure distribution and velocity field along the magnetohydrodynamic duct. Numerical simulations for pressure-velocity formulation show that the flow velocity of the electrolytic solution presents a maximum along the axial distance of the MHD channel. However, the results of the pressure analysis inside the electrolytic working fluid micropump taking into account the movement of the fluid show a noticeable increase in the exit of the duct. From Lorentz force analysis, we noticed that the oscillation amplitudes of the velocity and the pressure increase with the increasing of the current density and the magnetic flux density. So, the flow rate becomes more significant with the increase of magnetic and current density value. The obtained results confirm a directly influence of the external electromagnetic excitation and the chosen geometrical dimensions of the MHD duct on the velocity and pressure distribution in the investigated flow.

Acknowledgement

The authors would like to thank the referees for their helpful comments.

References

Anwari, M., Harada, N. and Takahashi, S., 2005, "Performance of a magnetohydrodynamic accelerator using air-plasma as working gas", Elsevier paper, *Energy Conversion Managem*ent, Vol. 4, pp. 2605-2613.

Ben Salah, N., 1999, "A Finite Element Method for the Fully-Coupled Magneto-hydrodynamics", Thesis in the Department of Mechanical Engineering, Concordia University, Montreal, Quebec, Canada.

Chorin, A.J., 1986, "Numerical solution of the Navier-Stokes equations", *Math. Comp.*, Vol. 22, pp. 745-762.

Cramer, K.R. & Pai, S., 1973, "Magnetofluid Dynamics For engineers and Applied Physicists", McGraw-Hill BooK.

Feynman, R.P., Leighton, R.B. and Sands, M., 1964, "The Feynman Lectures on Physics", Addison-Wesley, Reading, USA, Chapter 13-1.

Gerbeau, J.F. & Le Bris, C., 1997, "Existence of solution for a density dependant magnetohydrodynamic equation", *Advances in Differential Equations*, Vol. 2, No. 3, pp. 427-452.

Guermond, J.L. & Shen, J., 2003, "Velocity-correction projection methods for incompressible flows", *SIAM J. Numer. Anal.* Vol. 41, No. 1, pp. 112-134.

Harada, N., Ikewada, J. and Terasaki, Y., 2002, "Basic studies on an MHD accelerator", *AIAA paper* No.2175.

Heng, K.H., Huang, L., Wang, W. and Murphy, M.C., 1999, "Development of a diffuser/nozzle type micropump based on magnetohydrodynamic (MHD) principle", *SPIE*, Vol. 3877, pp. 66-73.

Holman, J.P., 1990, "Heat Transfer" (7th edition), Chapter 12, Special Topics in Heat Transfer, MacGraw-Hill Publishing Company, New York.

Homsy, A., Koster, S., Eijkel, J.C.T., Ven der Berg, A., Lucklum, F., Verpoorte, E. and de Rooij, N.F., 2005, "A high current density DC magnetohydrodynamic (MHD) micropump", *The Royal Society of Chemistry, Lab Chip*, Vol. 5, pp. 466-471.

Hunt, J.C.R., 1965, "Magnetohydrodynamic Flow in Rectangular Ducts" *J. Fluid Mechanics*, Vol. 21, No. 4, pp. 577-590.

Jang, J. and Lee, S.S., 2000, "Theoretical and experimental study of MHD (magnetohydrodynamic) micropump", *Sensors and Actuators*, Vol. 80, pp. 84-89.

Kadid, F.Z., Abdessemed, R. and Drid, S., 2004, "Study of the fluid flow in a MHD pump coupling finite element-finite volume computations", *Journal of Electrical Engineering*, Vol. 55, No. 11-12, pp. 301-305.

Kim, S.J., Lee, C.M. and Lee, S.J., 1997, "Experimental Investigation of Flow Characteristics of a magnetohydrodynamic (MHD) Duct of Fan-Shaped Cross Section", *KSME International Journal*, Vol. 11, No. 5, pp. 547-555.

Lee, D.S. & Choi, H., 2001, "Magnetohydrodynamic turbulence flow in a channel at low magnetic Reynolds number", *J. Fluid Mech*., Vol. 439, pp. 367.

Lemoff, A.V. & Lee, A.P., 2000, "An AC magnetohydrodynamic micropump", *Sensors and Actuators B*, Vol. 63, pp. 78-185.

Liu, X., Kiyoshi, T. and Takeda, M., 2006, "Simulation of a seawater MHD power generation system", *Cryogenics*, Vol. 46, pp. 362-366.

Shercliff, J.A., 1956, "The Flow of Conducting Fluids in Circular Pipes Under Transverse Magnetic Field", *J. Fluid Mechanics* , Vol. 1, pp. 644.

Temam, R., 1977, "Navier Stokes Equations", Stud. Math. Appl. 2, North-Holland, Amsterdam.

Temperley, D.J. & Todd, L., 1971, "The effects of wall conductivity in magnetohydrodynamic duct flow at high Hartmann number", *Proc. Cambridge Philosophical Society*, Vol. 69, pp. 337-351.

Tillack, M.S. & Morley, N.B., 1998, "MagnetoHydroDynamics", McGraw Hill, Standard Handbook for Electrical Engineers, 14th Edition.